Prediction of competitive adsorption on coal by a lattice DFT model

Adsorption (2010) 16: 37–46
DOI 10.1007/s10450-009-9197-2

PROCEEDINGS OF PBAST5

Prediction of competitive adsorption on coal by a lattice DFT model

Ronny Pini · Stefan Ottiger · Giuseppe Storti · Marco Mazzotti

Received: 31 July 2009 / Accepted: 13 October 2009 / Published online: 24 October 2009

Abstract Adsorption is one of the main mechanisms involved in the ECBM process, a technology where CO_2 (or flue gas, i.e. a CO_2/N_2 mixture) is injected into a deep coal bed, with the aim of storing CO_2 by simultaneously recovering CH_4. A detailed understanding of the microscopic adsorption process is therefore needed, as the latter controls the displacement process. A lattice DFT model, previously extended to mixtures, has been applied to predict the competitive adsorption behavior of CO_2, CH_4 and N_2 and of their mixtures in slit-shaped pores of 1.2 and 8 nm width. In particular, the effect of temperature, bulk composition and density on the resulting lattice pore profiles and on the lattice excess adsorption isotherms has been investigated. Important insights could be obtained; when approaching near critical conditions in the mesopores, a characteristic peak in the excess adsorption isotherm of CO_2 appears. The same effect could be observed neither for the other gases nor in the micropores. Moreover, in the case of mixtures, a depletion of the less adsorbed species close to the adsorbent surface is observed, which eventually results in negative lattice excess adsorption at high bulk densities.

Keywords Lattice DFT · ECBM · Competitive adsorption · Coal

R. Pini (✉) · S. Ottiger · M. Mazzotti
ETH Zurich, Institute of Process Engineering, Sonneggstrasse 3, 8092 Zurich, Switzerland
e-mail: pini@ipe.mavt.ethz.ch

M. Mazzotti
e-mail: marco.mazzotti@ipe.mavt.ethz.ch

G. Storti
Politecnico di Milano, Dipartimento di Chimica, Materiali e Ing. Chimica "Giulio Natta", Sede Mancinelli, Via Mancinelli 7, 20131 Milano, Italy

Notation

J	Overall number of lattice sites [–]
k	Boltzmann's constant [J/K]
N	Number of components in the mixture [–]
s	Entropy per molecule [J]
T	Temperature [K]
u	Internal energy per molecule [J]
U_{is}	Fluid-solid interaction energy [J]
y	Molar fraction [–]
z_0, z_1, z_2	Coordination numbers [–]

Greek letters

Γ^{lat}	Excess adsorption based on lattice occupancies [–]
ϵ	Fluid–fluid iteraction energy [J]
θ	Lattice occupancy (fractional coverage) [–]
ρ	Molar density [mol/L]
σ	Molecular collision diameter [Å]

Subscripts and superscripts

b	Bulk
c	Critical
i	Component i
j	Lattice site index
n	Component n

1 Introduction

In the global effort of reducing greenhouse gases emissions, Enhanced Coal Bed Methane (ECBM) recovery is an option under consideration for the geological storage of carbon dioxide (CO_2) (White et al. 2005; Mazzotti et al. 2009).

This process consists of injecting CO_2 into deep unmineable coal seams with concomitant recovery of the coal bed gas (mainly methane, CH_4). The recovered methane can be used for energy production, making CO_2 storage in coal beds an interesting option also from an economical point of view. This aspect, together with the high level of operational expertise gained in the past years for enhanced oil production, represents the premise for a faster implementation of the ECBM technology at a commercial scale compared to other scenarios for long term storage of CO_2 (White et al. 2005).

Adsorption plays a fundamental role in controlling the ECBM process: first, because the gas is stored in the coal seam both by adsorption on the coal surface and by penetration into the coal's solid matrix (absorption); estimates of the storage capacity in these reservoirs have therefore to rely on sorption measurements (Fitzgerald et al. 2005; Bae and Bhatia 2006; Day et al. 2008). Secondly, because ECBM is based on an adsorption (CO_2)/desorption (CH_4) process; studies have shown that it is indeed the dynamic of this displacement which affects the quantity and the quality of the recovered gas, and therefore the overall economics of the process (Jessen et al. 2008; Durucan and Shi 2009). Moreover, beside the knowledge of the adsorption behavior of a mixture of carbon dioxide and methane on coal, other binary systems, such as carbon dioxide-nitrogen or nitrogen-methane, or even ternary mixtures of them, may be promising to treat, being the direct injection of a flue gas instead of pure CO_2 into a coal seam an option under consideration (White et al. 2005).

A characterization study of coal for ECBM requires not only the measurement of pure and competitive sorption isotherms, but also a detailed understanding of the microscopic adsorption process, which e.g. can be attained by the use of models describing the actual nature of the adsorbent and taking into account interactions between the fluid molecules to be adsorbed (Fitzgerald et al. 2006; Kurniawan et al. 2006).

Statistical thermodynamics, and in particular the Density Functional Theory (DFT), offers a rigorous approach to describe adsorption in porous materials (Hill 1960). A particular application of this theory is the so-called lattice DFT model, whereby the pore space is discretized into sites in a lattice with a regular pattern and where the fluid molecules are confined. Each site of this lattice contains either a molecule or a vacancy, and interactions exist between the nearest neighbors, namely between fluid–fluid and fluid–solid molecules. Depending on the molecular size, the number of layers and the number of walls, pores of different sizes and shapes can be mimicked, namely one-dimensional slit pores, 2-dimensional channel pores and cubic cavities (Aranovich and Donohue 1997). In the past, this model has been used to investigate the behavior of supercritical CO_2 on different adsorbents with different pore size distributions (Aranovich and Donohue 1996; Hocker et al. 2003). More recently, we have extended the lattice DFT model to mixtures and we have applied it to coal, where experimentally obtained competitive adsorption isotherms of CO_2, CH_4 and N_2 on an Italian coal have been successfully described (Ottiger et al. 2008a, 2008b).

On the one hand, the simplification of the adsorbent pore structure and its representation as a family of pores with well defined size and shape may reduce the predictive capability of the lattice DFT model, in the case of adsorbents with heterogeneous pore structure and morphology, and complex pore connectivity. A more rigorous approach that overcomes these limitations is provided by the so-called reconstruction methods, which use stochastic simulation techniques to obtain a realistic structural model of the adsorbent to which molecular simulations can be applied (Palmer et al. 2009). On the other hand, by introducing information on the adsorbent pore size distribution, the lattice DFT model can be applied to a variety of adsorbent-adsorbate systems allowing to highlight those effects that are pore size dependent (Hocker et al. 2003). The lattice DFT model represents therefore a step forward compared to conventional approaches, such as semiempirical isotherm equations that provide only a macroscopic description of the adsorption equilibrium.

In the present paper, we use the lattice DFT model to investigate lattice occupancy profiles and lattice excess adsorption in simulated pores. This allows us to extend the knowledge on the adsorption behavior in coal further, as different conditions such as bulk density, fluid composition and temperature are analyzed in pores of different sizes, which are representative of typical micropores and mesopores.

2 Background

2.1 Modeling adsorption of mixtures through lattice DFT

The equations relating the density on a lattice site with the densities on its neighboring lattice sites and in the bulk have been derived by Ono and Kondo (1960) and they have been generalized to three dimensions by Aranovich and Donohue (1995, 1996, 1997, 1998). For the sake of clarity, the most important equations are summarized in the following for the case of a gas mixture (Ottiger et al. 2008b).

In particular, we consider the adsorption of a gas mixture of N components on an adsorbent consisting of a distribution of slit pores of given widths, with a hexagonal lattice arrangement. As shown in Fig. 1, in the hexagonal lattice each molecule has twelve nearest neighbors (six on its own plane, three above and three below). Moreover, each slit is confined by two identical flat and infinitely wide walls and its width corresponds to a J lattice (Fig. 1b and c). This

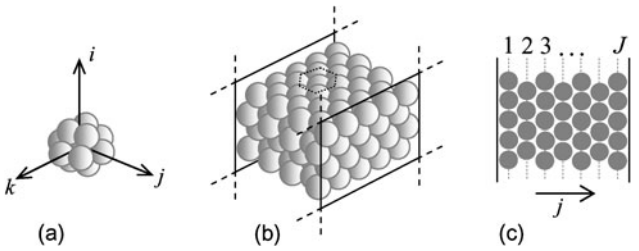

Fig. 1 Graphical representation of the slit pore lattice, with hexagonal geometry used in this study. (**a**) Unit cell of the hexagonal lattice; (**b**) three-dimensional slit pores; (**c**) one-dimensional (j-axis) representation

particular geometry allows to restrict the mathematical description of the problem to one dimension only. It is further assumed that the fluid molecules have the same size and that they all occupy a single lattice site, labeled with the index $j = 1, \ldots, J$. This assumption is supported by the fact that CO_2, CH_4 and N_2, i.e. the species considered in this study, have similar collision diameters, namely 4, 3.8 and 3.7 Å, respectively.

The derivation of the equations relating the density in each layer of the lattice to the density in the bulk starts by considering the exchange of a molecule of species i on a lattice site j inside the pore with a vacancy in the bulk under thermodynamic equilibrium, i.e.

$$\Delta u_i^j - T\Delta s_i^j = 0 \tag{1}$$

where T is the temperature and Δu_i^j and Δs_i^j represent the energy and entropy change associated to this reversible exchange, respectively.

By assuming that the two events are statistically independent, namely the one of having a molecule of species i on the lattice site j and the bulk site not occupied, and the other of having a molecule of species i in the bulk and the lattice site j empty, the following expression for the entropy change Δs_i^j is obtained

$$\Delta s_i^j = k \ln \frac{\theta_i^j (1-\theta^{\mathrm{b}})}{\theta_i^{\mathrm{b}} (1-\theta^j)} \tag{2}$$

where k is the Boltzmann constant; θ_i^j is the probability of a molecule of species i to be on site j; $\theta^j = \sum_i \theta_i^j$ is the probability of having site j occupied by a molecule of any species; θ_i^{b} is the probability of a molecule of species i to be in the bulk, i.e. occupying one or the other of the bulk sites that are assumed to be homogeneous; $\theta^{\mathrm{b}} = \sum_i \theta_i^{\mathrm{b}}$ is the probability of a molecule of any species to be in the bulk. Note that the probability θ can also be interpreted as a degree of lattice occupancy.

To obtain the change in energy Δu_i^j, two main assumptions are made. First, only the contribution from the configurational energy is considered and therefore this change is given by the sum of the simultaneous interactions among all pairs of molecules (pairwise additivity). Secondly, these pair interactions are restricted to those between nearest neighbors. Therefore, for a site j which is not adjacent to the wall the term Δu_i^j is given by

$$\Delta u_i^j = -\sum_{n=1}^{N} \epsilon_{in} \left(z_2 \theta_n^{j-1} + z_2 \theta_n^{j+1} + z_1 \theta_n^j - z_0 \theta_n^{\mathrm{b}} \right) \tag{3}$$

where ϵ_{in} represents the fluid–fluid interaction energy between nearest neighboring molecules of species i and n. The parameter z_0 is the coordination number in the bulk, z_1 the one within any layer and $z_2 = (z_0 - z_1)/2$. For the hexagonal lattice geometry considered here $z_0 = 12$, $z_1 = 6$, and $z_2 = 3$. The Ono-Kondo lattice equation, i.e. (1), can therefore be written as follows:

$$\sum_{n=1}^{N} \epsilon_{in} \left(z_2 \theta_n^{j-1} + z_2 \theta_n^{j+1} + z_1 \theta_n^j - z_0 \theta_n^{\mathrm{b}} \right) + kT \ln \frac{\theta_i^j (1-\theta^{\mathrm{b}})}{\theta_i^{\mathrm{b}} (1-\theta^j)} = 0 \quad \text{for } j = 2, \ldots, J-1 \tag{4}$$

Accordingly, in the case of a molecule on the lattice site 1 or J, i.e. those adjacent to the pore walls, the following equations are obtained:

$$\begin{aligned} &U_{is} + \sum_{n=1}^{N} \epsilon_{in} \left(z_2 \theta_n^{j+1} + z_1 \theta_n^j - z_0 \theta_n^{\mathrm{b}} \right) + kT \ln \frac{\theta_i^j (1-\theta^{\mathrm{b}})}{\theta_i^{\mathrm{b}} (1-\theta^j)} = 0 \quad \text{for } j = 1 \\ &U_{is} + \sum_{n=1}^{N} \epsilon_{in} \left(z_2 \theta_n^{j-1} + z_1 \theta_n^j - z_0 \theta_n^{\mathrm{b}} \right) + kT \ln \frac{\theta_i^j (1-\theta^{\mathrm{b}})}{\theta_i^{\mathrm{b}} (1-\theta^j)} = 0 \quad \text{for } j = J \end{aligned} \tag{5}$$

where U_{is} is the fluid-wall interaction energy for species i.

Equations (4) and (5) can be written for every species $i = 1, \ldots, N$; once temperature T, bulk occupancy θ^{b}, bulk composition $y_i^{\mathrm{b}} = \theta_i^{\mathrm{b}}/\theta^{\mathrm{b}}$, interaction energies U_{is} and ϵ_{in} are given, the resulting set of NJ coupled, nonlinear algebraic equations can be solved numerically for the unknown lattice occupancies θ_i^j. From the calculated lattice occupancy profile in the slit pore, the lattice excess adsorption Γ_i^{lat} is readily obtained:

$$\Gamma_i^{\mathrm{lat}} = \sum_{j=1}^{J} \left(\theta_i^j - \theta_i^{\mathrm{b}} \right) \tag{6}$$

2.2 Matching DFT model and physical reality

To describe adsorption data obtained experimentally, a link needs to be established between the results predicted by the lattice DFT model and the physical reality. In other words, one has to go from the dimensionless excess adsorption based on lattice occupancies Γ_i^{lat}, to the excess adsorption defined in typical adsorption units, such as moles of adsorbate per unit mass adsorbent. To achieve this some issues need to be addressed, which are summarized in the following (Ottiger et al. 2008b).

A so-called mapping function is defined, that relates the total lattice occupancy, $\theta = \sum_i \sum_j \theta_i^j$, to the total molar fluid density ρ, i.e $\rho = g(\theta)$. This function fulfills the following constraints: the density is zero at $\theta = 0$, and it reaches its maximum value as the lattice sites are all occupied, i.e. $\rho = \rho^{\max}$ at $\theta = 1$. For pure fluids, this value is component specific and can be estimated from the number density of close-packed spheres, i.e. $\sqrt{2}/\sigma_i^3$. Moreover, the critical density ρ^{c} of the fluid is reached at $\theta = 0.5$, which is as general feature of Ising type lattice models based on simple nearest-neighbor interactions and a fixed lattice spacing (Hill 1956). Note, that both maximum and critical density of the fluid mixture depend on its composition and they can be estimated from the pure components densities by applying appropriate weighting rules. Moreover, the molar densities of each adsorbate ρ_i in the mixture can be obtained as:

$$\rho_i = \frac{\theta_i}{\theta}\rho \tag{7}$$

being the mole fraction of the fluid mixture defined as $y_i = \theta_i/\theta$.

A further step in the description of the real system is achieved by including information on the pore structure of the adsorbent in the lattice DFT model. In particular, the pore size distribution is discretized into a finite number of families of pores with a specific size; in addition, a given weight is attributed to each of them, corresponding to their specific volume in the real pore size distribution.

2.3 Adsorption of CO_2, CH_4 and N_2 on coal

In a previous publication (Ottiger et al. 2008b), competitive high-pressure adsorption data of CO_2, CH_4 and N_2 on an Italian coal have been described using the same lattice DFT model presented in Sect. 2.1. Three families of pores have been chosen to be representative of the coal real pore size distribution: two in the micropore region, that is 1.2 and 1.6 nm, and one in the mesopore region, that is 20 nm. By assuming a molecule diameter of 4 Å (see Sect. 2.1), they are implemented in the lattice DFT model as slit-pores with 3, 4 and 50 layers, respectively. It is worth noting, that this representation of the pore structure is a strong simplification of the reality of coal. First, because coal possesses a highly heterogeneous pore structure, including many different pore sizes, shapes and complex wall topologies (Stach 1982). Moreover, many others factors influence the adsorption phenomena, such as the presence of functional groups (Van Krevelen 1981), which can not be included by considering a simple slit-like pore geometry. Finally, the thermal history undergone by the coal during its formation has determined its final composition and micro-structural features, allowing to classify it according to a specific rank. As a consequence, all the factors mentioned above may differ from coal to coal, making the analysis of the adsorption behavior directly dependent on the type of coal considered.

Table 1 Physical properties of the pure adsorbates

Fluid	T_{c} [K]	P_{c} [bar]	ρ^{c} [mol/L]	σ [Å]
CO_2	304.1	73.7	10.63	4.0
CH_4	190.6	46.0	10.14	3.8
N_2	126.2	34.0	11.18	3.7

Table 2 Parameter values used in the lattice DFT model for the adsorption of pure and multicomponent mixtures of CO_2, CH_4 and N_2 on coal

ϵ_{in}/k [K]	CO_2	CH_4	N_2	U_{is}/k [K]
CO_2	−101.4	−80.3	−65.3	−1427
CH_4		−63.5	−51.7	−1122
N_2			−42.1	−1016

As mentioned in Sect. 2.1, values for the fluid–fluid and fluid–solid interaction energies are required to solve the lattice DFT model. The fluid–fluid interaction energy ϵ_{ii} between same molecules is chosen so as the real fluid and the lattice fluid have the same critical temperature, i.e. $|\epsilon_{ii}| = 4kT_{\text{c}}/z_0$. In the case of mixtures, the fluid–fluid interaction energy ϵ_{in} between different molecules is estimated by applying a classical geometric mean to the interaction energies of the pure fluids, i.e. $|\epsilon_{in}| = \sqrt{|\epsilon_{ii}||\epsilon_{nn}|}$. The values of the fluid–solid interaction energies U_{is} have been obtained by fitting the experimental adsorption data (Ottiger et al. 2008b). Values for the pure components physical properties as well as for the energetic parameters are summarized in Tables 1 and 2, respectively. It is worth noting, that when a coal of different rank is considered, the same procedure can be applied, by modifying only the coal-specific model parameters, namely its pore size distribution and the fluid solid-interaction energy, which account for the different structural and chemical characteristics of the coal.

Finally, an important remark has to be made concerning the gas uptake mechanism, which in the case of coal is a combination of adsorption on its porous surface and absorption into its solid matrix. The latter mechanism is associated with a volumetric change (swelling) of the coal matrix and it

is not automatically present in the lattice DFT model; to take it into account we assume that the volume of the three-layer pores is different for every component i. In particular, this volume has been let to be completely accessible for CO_2, as the coal pore size distribution has been measured with CO_2 as well, whereas for CH_4 and N_2, for which absorption is known to be smaller (St. George and Barakat 2001), it has been reduced. In other words, a larger volume for adsorption is used in the model to compensate for a larger absorption. The fraction of this accessible pore volume to the different gases has been selected by fitting the experimental data, thus obtaining the values of 100% for CO_2, 49% for CH_4 and 14% for N_2.

3 Results and discussion

Once calibrated by fitting it to the experimental data, the lattice DFT model represents a powerful tool to be used to improve the understanding of the competitive adsorption behavior in coal. In the next sections, a step forward in this analysis is carried out by looking at lattice occupancy profiles and lattice excess adsorption isotherms obtained for the adsorption of pure, binary and ternary mixtures of CO_2, CH_4 and N_2 in simulated coal pores with different sizes and under different conditions of bulk density, fluid composition and temperature. In particular, slit-pores with 3 and 20 layers are considered, corresponding to a micropore (1.2 nm) and a mesopore (8 nm), respectively. Mesopores with 20 layers have been chosen instead of 50-layer pores for the sake of clarity, since the same effects have been observed, but their illustration with 20-layer pores is more effective than with 50-layer pores.

3.1 Pure fluids

Figure 2 shows the lattice occupancy profiles of CO_2, CH_4 and N_2 at 45 °C and for three different bulk occupancies ($\theta^b = 0.25$, 0.5 and 0.75) in two types of pores, namely in a 3 and in a 20-layer pore. It can be seen that in both cases the local values of the lattice occupancy θ^j increase steeply close to the pore walls. This attraction by the wall is essentially local for CH_4 and N_2, whereas for CO_2 it has a long-range character and it extends relatively far into the pore. This effect is due to the experimental temperature, which for CO_2 is much closer to its critical temperature than for the other two fluids. In fact, the reduced temperatures T/T_c are 1.05, 1.67 and 2.52 for CO_2, CH_4 and N_2, respectively. Moreover, in the mesopore the lattice occupancy stays at its bulk value in the center of the pores, whereas in the smaller micropore the value of the lattice occupancy is always larger than the bulk occupancy. Again, this effect is much more evident for CO_2 compared to CH_4 and N_2, due to the larger

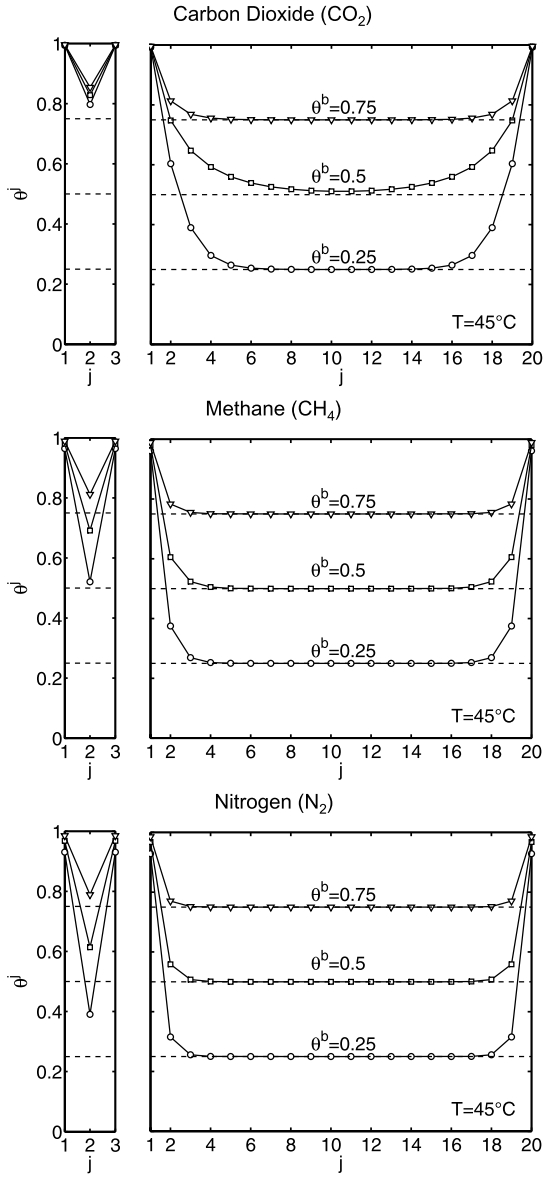

Fig. 2 Pure fluid lattice occupancy profiles of CO_2, CH_4 and N_2 at 45 °C in a 3 and 20-layer slit pore at different bulk occupancies θ^b

adsorption strength of the former compared to the other two fluids, which is reflected by the value of the fluid–solid interaction energies U_{is} (see Table 2).

3.1.1 *Effect of temperature*

The effect of the temperature on adsorption as predicted by the lattice DFT model for different pore sizes is illustrated in Fig. 3, where the lattice excess adsorption isotherms in a 3- and 20-layer slit pore are shown at 32, 45 and 70 °C for CO_2, CH_4 and N_2, respectively. A first remark to be made is that all the isotherms fulfill the limit that $\Gamma^{lat} \to 0$ as $\theta^b \to 0$ or $\theta^b \to 1$, as given by (6) for the pure components. Moreover, for all gases and in both pores, a decrease in temperature

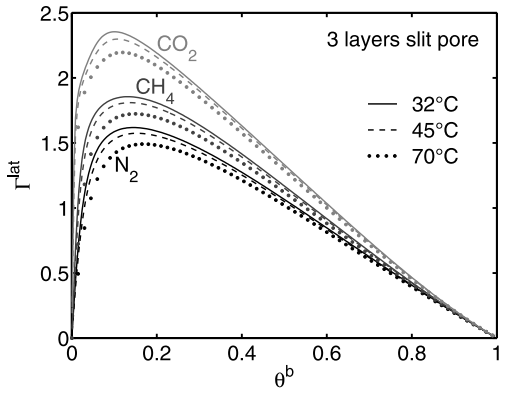

(a) 3-layer slit pore

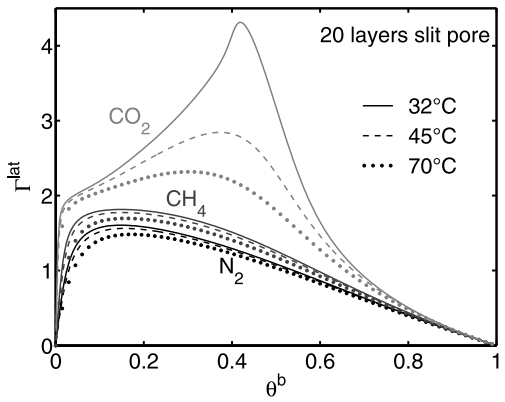

(b) 20-layer slit pore

Fig. 3 Effect of temperature T on the lattice excess adsorption Γ^{lat} as a function of the bulk lattice occupancy θ^{b} for pure CO_2, CH_4 and N_2. Slit pore size: (**a**) 3 layers; (**b**) 20 layers

leads to an increases in the lattice occupancy, corresponding to an increase in adsorption, as expected since adsorption is exothermic.

In the case of the 3-layer pore, the excess isotherms are characterized by a steep increase at low bulk occupancies, a maximum and a linear decrease as the bulk occupancy increases further. It can also be observed that for all gases the position of the maximum of Γ^{lat} shifts towards higher values of θ^{b} with increasing temperatures, in accordance with other studies (Ustinov et al. 2002; Hocker et al. 2003). Now let us consider the isotherms obtained for the 20-layer pore. It can be readily observed that for CH_4 and N_2 the isotherms are very similar to those predicted for the micropore case. On the contrary, in the case of CO_2 the isotherms look very different and are characterized by a maximum at larger bulk occupancies. Note that this maximum lies always below a bulk occupancy $\theta^{\text{b}} = 0.5$; this value corresponds to the critical density of the lattice gas (see Sect. 2.2). With decreasing temperature the height of this maximum increases and the isotherm exhibits a marked peak. As explained in previous publications, this behavior is particularly marked for CO_2 and is interpreted as a propagation of the attractive potential exerted by the pore walls into the center of the pore (Aranovich and Donohue 1997; Hocker et al. 2003). This is made possible by the increase in correlation length in a fluid at near-critical conditions, as it is the case here, being the reduced temperatures of CO_2, $T/T_{\text{c}} = 1.003$, 1.05 and 1.13, respectively. On the contrary, at conditions far above the critical temperature, the shape of the lattice excess adsorption isotherm is only slightly influenced by the choice of the specific pore size and fluid temperature.

3.2 Binary mixtures

3.2.1 CO_2/CH_4

Let us first focus on the mixtures containing CO_2 and CH_4, which are the two main species in the ECBM operation. Figure 4 shows the individual and total lattice excess adsorption Γ_i^{lat} and Γ^{lat} in the 20-layer pore as a function of the bulk lattice occupancy at 45 °C for a lattice with three different bulk equilibrium compositions, namely 25% CO_2:75% CH_4, 50% CO_2:50% CH_4 and 75% CO_2:25% CH_4. As expected the adsorption of each component i increases with increasing concentration of the specific component in the bulk phase. Moreover, over the whole range of bulk occupancies and for all bulk compositions, CO_2 is the most adsorbed component. Even if the concentration of CO_2 in the bulk is lowered, the adsorption competition stays in favor of CO_2; as an example, for the mixture with bulk composition 25% CO_2:75% CH_4 and bulk occupancy $\theta^{\text{b}} = 0.4$, CO_2 accounts for 60% of the total amount adsorbed. The main reason for this behavior lies in the value of the fluid–solid interaction value, which is higher for CO_2 (−1427 K) as compared to CH_4 (−1122 K).

Interestingly, while the excess isotherm for the total adsorption fulfill the limit that $\Gamma^{\text{lat}} \to 0$ as $\theta^{\text{b}} \to 0$ or $\theta^{\text{b}} \to 1$, the individual adsorption isotherms satisfy this constraint only for $\theta^{\text{b}} \to 0$. In fact, while the CO_2 excess isotherm is always positive, the CH_4 isotherm crosses the horizontal axis and becomes negative at large bulk occupancies. This behavior can be best understood by looking at the lattice occupancy profiles in the pore, which are shown in Fig. 5 for pure CO_2, for pure CH_4 and for their mixtures at a bulk lattice occupancy of $\theta^{\text{b}} = 0.6$. Here, the effect of competitive adsorption can be clearly seen: on the one hand, the lattice occupancy of the more strongly adsorbed component (CO_2) increases significantly close to the wall and reaches values almost as high as in the pure case. On the other hand, for the less adsorbing CH_4, this increase close to the wall can be seen only in the pure case, whereas for the mixtures the local occupancy flattens out or it even decreases and eventually becomes lower than the corresponding bulk lattice occupancy θ_i^{b}. As an example, for an equimolar bulk composition (50% CO_2:50% CH_4) corresponding to $\theta^{\text{b}}_{\text{CH}_4} = \theta^{\text{b}}_{\text{CO}_2} = 0.3$,

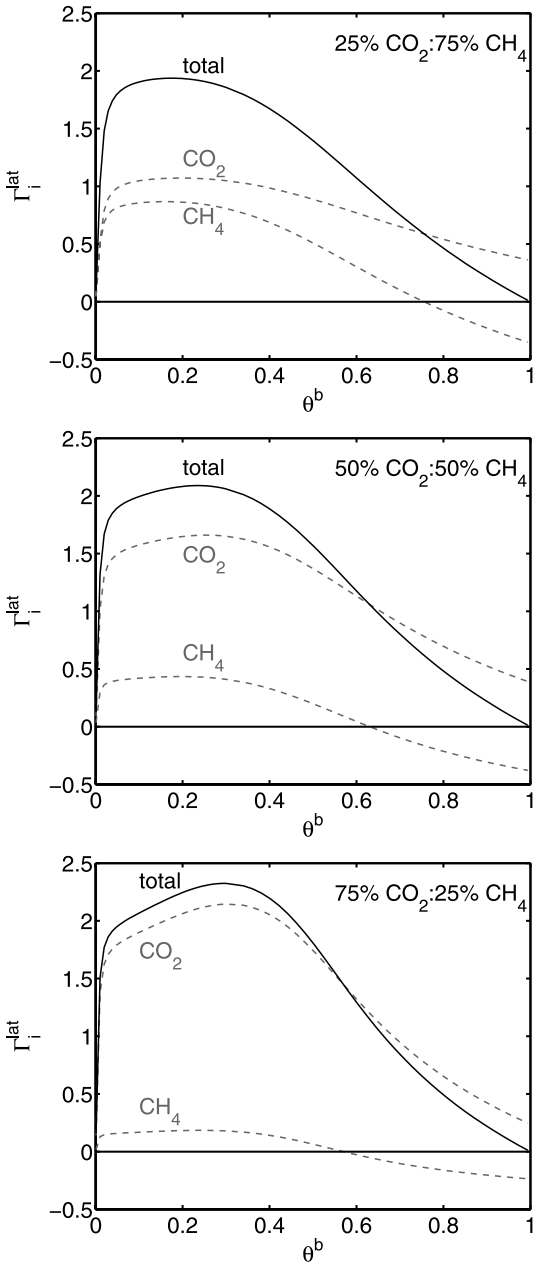

Fig. 4 Individual and total lattice excess adsorption Γ_i^{lat} at 45 °C in a 20-layer pore as a function of the bulk lattice occupancy θ^{b} for the three binary CO_2/CH_4 mixtures

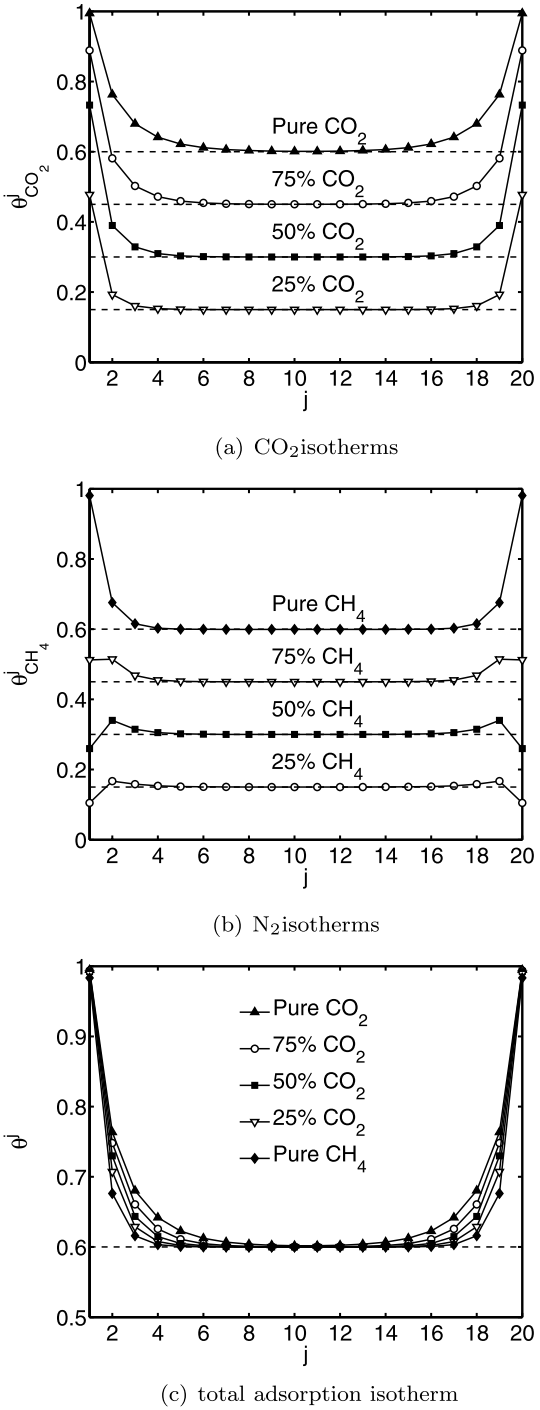

Fig. 5 Lattice occupancy profiles of (**a**) CO_2, (**b**) CH_4 and total (**c**) for pure CO_2, pure N_2 and three binary mixtures of them at 45 °C in a 20-layer pore at a mixture bulk occupancy $\theta^{\text{b}} = 0.6$. *Horizontal dash-dot lines* correspond to the individual bulk lattice occupancy θ_i^{b}

the lattice occupancy at the wall site $j = 1$, reaches 0.74 for CO_2, but only 0.26 for CH_4, the latter being lower than its bulk lattice occupancy. When this depletion in the occupancy of the less adsorbing component is large enough, it leads to a negative excess adsorption Γ_i^{lat} at high bulk lattice occupancies, as it can be seen in (6).

3.2.2 CO_2/N_2 and CH_4/N_2

The analysis of the adsorption behavior can be extended to other binary systems involving the gases of interest for the ECBM operation, namely CO_2/N_2 and CH_4/N_2. The former corresponds to the case where the difference in fluid–solid interaction energies of the two species involved is the largest, whereas for the latter this difference is the smallest, thus leading to a stronger and a weaker competitive adsorp-

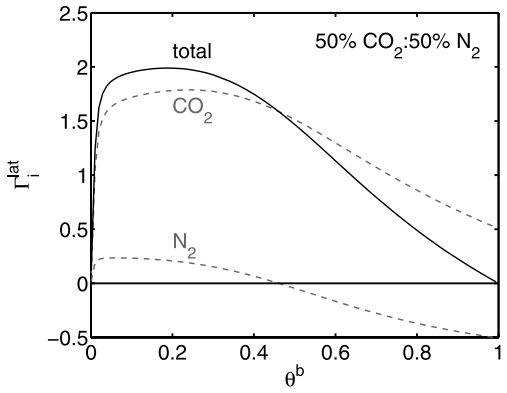

(a) Lattice excess isotherms

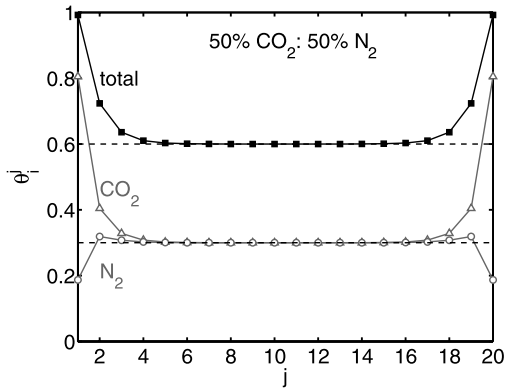

(b) Lattice occupancy profiles

Fig. 6 Competitive adsorption of a 50% CO_2:50% N_2 mixture at 45 °C in a 20-layer pore: (**a**) Individual and total lattice excess adsorption Γ_i^{lat} as a function of the bulk lattice occupancy θ^{b}. (**b**) Individual lattice occupancy profiles at a mixture bulk occupancy $\theta^{\text{b}} = 0.6$

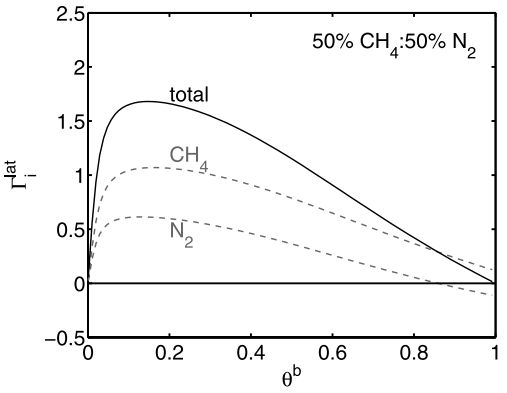

(a) Lattice excess isotherms

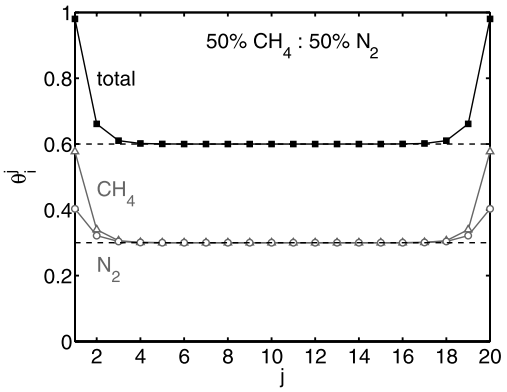

(b) Lattice occupancy profiles

Fig. 7 Competitive adsorption of a 50% CH_4:50% N_2 mixture at 45 °C in a 20-layer pore: (**a**) Individual and total lattice excess adsorption Γ_i^{lat} as a function of the bulk lattice occupancy θ^{b}. (**b**) Individual lattice occupancy profiles at a mixture bulk occupancy $\theta^{\text{b}} = 0.6$

tion between the two components, respectively. The model results confirm these expectations and are shown in Figs. 6 and 7 for CO_2/N_2 and CH_4/N_2 mixtures, respectively. In particular, Fig. 6a shows individual and total lattice excess adsorption Γ_i^{lat} and Γ^{lat} in the 20-layer pore as a function of the bulk lattice occupancy at 45 °C for a bulk lattice composition of 50% CO_2:50% N_2. It can be seen that adsorption is strongly in favor of CO_2 and as consequence the excess lattice adsorption of N_2 becomes negative already at a bulk occupancy of 0.5. The corresponding lattice occupancy profiles calculated for a bulk lattice occupancy of $\theta^{\text{b}} = 0.6$ are shown in Fig. 6b, where it can be seen that the depletion of N_2 at the adsorbent surface is much more marked compared to the CO_2/CH_4 case.

In the case of the CH_4/N_2 mixtures, the competitive adsorption effect is still present, but in a much less pronounced manner. The individual lattice excess adsorption isotherms shown in Fig. 7a are in fact always positive until a very high bulk occupancy is reached ($\theta^{\text{b}} = 0.82$). A similar conclusion can be drawn from he lattice occupancy profiles shown in Fig. 7b, where for both species the local occupancy θ_i^j increases close to the slit-pore walls.

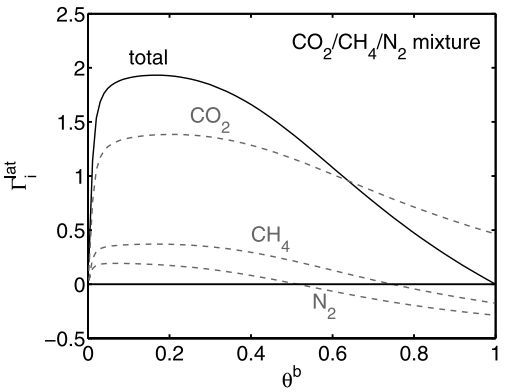

Fig. 8 Individual and total lattice excess adsorption Γ_i^{lat} at 45 °C in a 20-layer pore as a function of the bulk lattice occupancy θ^{b} for a ternary mixture of composition 33.3% CO_2, 33.3% CH_4 and 33.4% N_2

3.3 Ternary mixture

Figure 8 shows the individual and total lattice excess adsorption Γ_i^{lat} and Γ^{lat} in the 20-layer pore as a function of

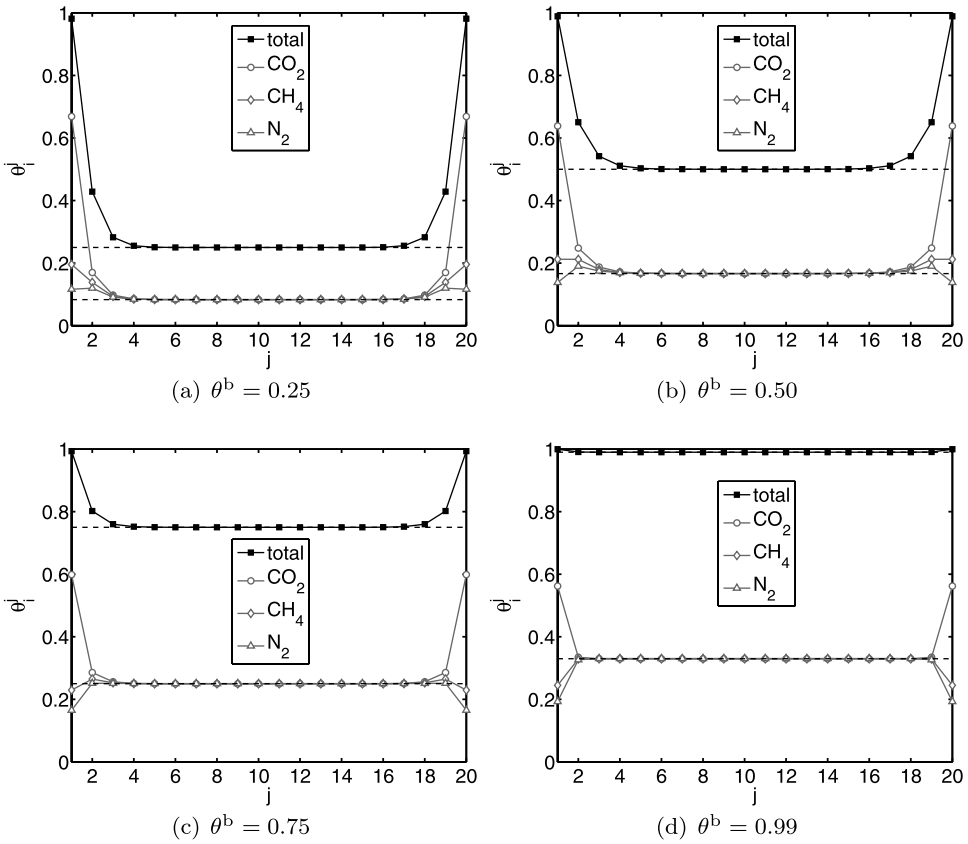

Fig. 9 Lattice occupancy profiles at different mixture bulk occupancies θ^b of a ternary mixture of composition 33.3% CO_2, 33.3% CH_4 and 33.4% N_2 at 45 °C in a 20-layer pore

the bulk lattice occupancy at 45 °C for a ternary mixture, whose bulk equilibrium composition is 33.3% CO_2:33.3% CH_4:33.4% N_2. As expected, the results are a combination of the observations made above for the different binary mixtures: CO_2 shows the strongest adsorption, compared to CH_4 and N_2, for which the competition for adsorption is much weaker; in addition for CH_4 and N_2, the excess lattice occupancy becomes negative at $\theta^b = 0.75$ and 0.5, respectively. In Fig. 9, the lattice occupancy profiles are shown for four different values of θ^b. It can be seen that the depletion at the surface for the less stronger adsorbing components increases with increasing bulk occupancy. At low bulk lattice occupancy, e.g. $\theta^b = 0.25$, it can be seen only for nitrogen, whereas from $\theta^b = 0.5$ it affects methane as well. Note that at $\theta^b = 0.99$, where the pore is almost completely filled, CO_2 is preferentially adsorbed over CH_4 and even more significantly over N_2, leading to θ_i^j values at the surface larger than their corresponding values in the bulk for CO_2 and smaller for CH_4 and N_2, respectively.

4 Conclusion

The knowledge of the adsorption characteristics of coal bed gases on coal is especially important in the description of the ECBM process, whereby CO_2 or a flue gas (a CO_2/N_2 mixture) is injected into a deep coal bed, with the aim of storing CO_2 by simultaneously recovering CH_4. The lattice DFT model has been shown to be a valuable approach for the description of supercritical gas adsorption in several porous adsorbents (Aranovich and Donohue 1996; Hocker et al. 2003). Moreover, it can be readily extended to mixtures, as it has been shown in a recent work, where the lattice DFT model has been successfully applied to describe experimentally obtained competitive adsorption isotherms of CO_2, CH_4 and N_2 on an Italian coal (Ottiger et al. 2008b). Slit-pores with 3, 4 and 50 layers have been chosen to be representative of the real pore size distribution of coal. The fluid–solid interaction energies and the fraction of 3-layers pore accessible to the different gases have been used as fitting parameters. The latter has been introduced in order to account in the DFT model also for gas absorption into the coal solid matrix, which together with gas adsorption, is the main mechanism for gas storage in coal beds.

Beside the successful description of the obtained excess adsorption isotherms, which in principle can be achieved also with simpler, semiempirical models, the lattice DFT model allows to obtain important insights on the adsorption mechanisms, as it includes information on the pore structure of the adsorbent and accounts for fluid–fluid and fluid–solid interactions. In this work, the analysis of the competitive adsorption behavior in coal has been extended by

investigating the influence of different parameters such as temperature, bulk composition and pore size on the resulting lattice pore profiles and on the lattice excess adsorption isotherms. In particular, the adsorption of pure, binary and ternary mixtures of CO_2, CH_4 and N_2 into slit-pores with 3 (micropore) and 20 (mesopore) layers has been studied. A characteristic behavior of CO_2 in the mesopore could be highlighted, which takes place in the mesopores when critical conditions are approached and which translates into a marked peak in the excess adsorption isotherm. Moreover, in the case of mixtures, the model results showed that close to the adsorbent surface competitive adsorption between different species leads to a depletion of the less adsorbed species resulting in even negative lattice excess adsorption at high bulk occupancies. The benefits of the lattice DFT model have to be evaluated considering also its limitations, i.e. one has to keep in mind the simplifications that have been introduced and that may limit the predictive capability of this approach. As already discussed, the key simplifications of the model are the definition of a so-called mapping function to relate the lattice variables (fractional coverage) to the experimental variables (excess adsorbed amount), the adoption of a unique pore structure and shape, the use of a integer number of layers in the pore and the assumption that the different gas molecules have the same size and shape. However, the introduction of information on the adsorbent pore size distribution, which is achieved by applying the lattice DFT model, offers the possibility to highlight those peculiarities of the adsorption phenomenon that are related to the size of the pores and that are particularly evident at near-critical conditions (Hocker et al. 2003). Therefore we consider this approach, although simple to implement, very useful and instructive from an adsorption fundamentals point of view.

References

Aranovich, G.L., Donohue, M.D.: Adsorption-isotherms for microporous adsorbents. Carbon **33**(10), 1369–1375 (1995)

Aranovich, G.L., Donohue, M.D.: Adsorption of supercritical fluids. J. Colloid Interface Sci. **180**(2), 537–541 (1996)

Aranovich, G.L., Donohue, M.D.: Predictions of multilayer adsorption using lattice theory. J. Colloid Interface Sci. **189**(1), 101–108 (1997)

Aranovich, G., Donohue, M.: Analysis of adsorption isotherms: Lattice theory predictions, classification of isotherms for gas-solid equilibria, and similarities in gas and liquid adsorption behavior. J. Colloid Interface Sci. **200**(2), 273–290 (1998)

Bae, J.S., Bhatia, S.K.: High-pressure adsorption of methane and carbon dioxide on coal. Energy Fuels **20**(6), 2599–2607 (2006)

Day, S., Duffy, G., Sakurovs, R., Weir, S.: Effect of coal properties on CO_2 sorption capacity under supercritical conditions. Int. J. Greenhouse Gas Control **2**(3), 342–352 (2008)

Durucan, S., Shi, J.Q.: Improving the CO_2 well injectivity and enhanced coalbed methane production performance in coal seams. Int. J. Coal Geol. **77**(1–2), 214–221 (2009)

Fitzgerald, J.E., Pan, Z., Sudibandriyo, M., Robinson, R.L., Gasem, K.A.M., Reeves, S.: Adsorption of methane, nitrogen, carbon dioxide and their mixtures on wet Tiffany coal. Fuel **84**(18), 2351–2363 (2005)

Fitzgerald, J.E., Robinson, R.L., Gasem, K.A.M.: Modeling high-pressure adsorption of gas mixtures on activated carbon and coal using a simplified local-density model. Langmuir **22**(23), 9610–9618 (2006)

Hill, T.L.: Statistical Mechanics: Principles and Selected Applications. McGraw-Hill, New York (1956)

Hill, T.L.: Introduction to statistical Thermodynamics. Addison-Wesley Series in Chemistry. Addison-Wesley, Reading (1960)

Hocker, T., Rajendran, A., Mazzotti, M.: Measuring and modeling supercritical adsorption in porous solids. Carbon dioxide on 13X zeolite and on silica gel. Langmuir **19**(4), 1254–1267 (2003)

Jessen, K., Tang, G.Q., Kovscek, A.: Laboratory and simulation investigation of enhanced coalbed methane recovery by gas injection. Transp. Porous Media **73**(2), 141–159 (2008)

Kurniawan, Y., Bhatia, S.K., Rudolph, V.: Simulation of binary mixture adsorption of methane and CO_2 at supercritical conditions in carbons. AlChE J. **52**(3), 957–967 (2006)

Mazzotti, M., Pini, R., Storti, G.: Enhanced coal bed methane recovery. J. Supercrit. Fluids **47**(3), 619–627 (2009)

Ono, S., Kondo, S.: Molecular Theory of Surface Tension in Liquids. Springer, Göttingen (1960)

Ottiger, S., Pini, R., Storti, G., Mazzotti, M.: Competitive adsorption equilibria of CO_2 and CH_4 on a dry coal. Adsorption **14**(4–5), 539–556 (2008a)

Ottiger, S., Pini, R., Storti, G., Mazzotti, M.: Measuring and modeling the competitive adsorption of CO_2, CH_4 and N_2 on a dry coal. Langmuir **24**(17), 9531–9540 (2008b)

Palmer, J.C., Brennan, J.K., Hurley, M.M., Balboa, A., Gubbins, K.E.: Detailed structural models for activated carbons from molecular simulation. Carbon **47**(12), 2904–2913 (2009)

St. George, J.D., Barakat, M.A.: The change in effective stress associated with shrinkage from gas desorption in coal. Int. J. Coal Geol. **45**(2–3), 105–113 (2001)

Stach, E.: In: Stach, E., Mackowsky, M.Th., Teichmüller, M., Taylor, G.H., Chandra, D., Teichmüller, D. (eds.) Stach's Textbook of Coal Petrology. Gebrüder Borntraeger, Berlin/Stuttgart (1982)

Ustinov, E.A., Do, D.D., Herbst, A., Staudt, R., Harting, P.: Modeling of gas adsorption equilibrium over a wide range of pressure: A thermodynamic approach based on equation of state. J. Colloid Interface Sci. **250**(1), 49–62 (2002)

Van Krevelen, D.W.: Coal: typology - chemistry - physics - constitution. In: Anderson, L. (ed.) Coal Science and Technology. Elsevier, Amsterdam (1981)

White, C.M., Smith, D.H., Jones, K.L., Goodman, A.L., Jikich, S.A., LaCount, R.B., DuBose, S.B., Ozdemir, E., Morsi, B.I., Schroeder, K.T.: Sequestration of carbon dioxide in coal with enhanced coalbed methane recovery - A review. Energy Fuels **19**(3), 659–724 (2005)